Palm Vein Recognition Using a High Dynamic Range Approach

Emanuela Piciucco [1*], *Emanuele Maiorana* [1], *Patrizio Campisi* [1]

[1] *Department of Engineering, Section of Applied Electronics, Roma Tre University, Via Vito Volterra 62, 00146, Rome, Italy*
** E-mail: emanuela.piciucco@uniroma3.it*

Abstract: In this paper we propose a novel approach for palm vein recognition relying on high dynamic range (HDR) imaging. Specifically, we speculate that the exploitation of multiple-exposure vein images guarantees better recognition performance than a baseline system relying on single-exposure acquisitions. In order to verify our assumptions, a multiple-exposure dataset is collected from 86 subjects, with twelve sets of palm vein images captured for each user. Each set is composed by five images, acquired at different exposures, which can be fused to generate a HDR representation of the actual vein pattern. Local binary pattern (LBP) and local derivative pattern (LDP) are employed to extract features from single-exposure images, raw HDR images, and tone-mapped HDR images. The obtained experimental results show that significant performance improvement can be achieved when discriminative features are extracted from HDR contents, with respect to the use of single-exposure images.

1 Introduction

In recent years, automatic human identification has become one of the most requested tasks in the field of commercial applications, such as e-commerce, ATM cash withdrawals, smartphone unlocking, and government applications, such as border and security controls. The most demanding requirement all these systems share is the security they need to provide. Possible ways to automatically authenticate users is through knowledge-based systems, e.g. passwords, that can be stolen or forgotten, or through token-based systems, e.g. smart cards, that can be lost or robbed. In order to overcome the security issues affecting the aforementioned authentication modalities, biometrics, that is automatic recognition of individuals based on their physiological and/or behavioral characteristics, is extensively employed in many applications [1].

Among the existing biometric identifiers, one of the emerging biometric trait is vein pattern. Recently, the use of vein patterns for biometric recognition is being attracting more and more interest from both the industries and the research community [2]. In fact, the exploitation of such traits guarantees several advantages compared to the use of other biometric identifiers [3]. First, vein patterns are not exposed biometric characteristics, imaged using near-infrared (NIR) cameras and illumination, therefore difficult to steal and replicate. In addition, vein-based acquisition devices are contactless, thus entailing convenience for the users. Moreover, liveness detection is easily performable. On the other hand, vein-pattern images are often characterized by low contrast and poor definition, due to the subcutaneous placement of the veins, thus making vein-related feature extraction a challenging process [4].

In our work, a novel approach for palm vein recognition is proposed. In order to overcome the disadvantages due to the low contrast of the acquired vein patterns, we rely on high dynamic range (HDR) imaging techniques [5–7], thus following a sensor-level fusion approach. Pictures of the same vein structure are acquired with a constant light source but setting different exposure times and then combined in order to generate images with an improved quality. In detail, pictures where the ratio between luminance of the lightest and darkest areas is higher than the one obtained in a single-exposure image, namely low dynamic range (LDR) image, can be generated by the HDR processing. As extensively shown in Section 5, this may allow better feature extraction, guaranteeing significant improvements of the recognition performance.

The rest of this paper is organized as follows: after presenting the state of the art of palm vein recognition in Section 2, a brief overview of the image quality issues in vein recognition systems and of HDR imaging is given in Section 3. Section 4 describes the employed palm vein recognition system, including preprocessing, feature extraction, and matching techniques. Section 5 explains the setup of our experimental study and provides the obtained results. A comparison between the performance achievable through the proposed approach, and what can be obtained using different image enhancement methods and a score-level fusion approach, is also given. Eventually, some conclusions are drawn in Section 6.

2 Palm vein recognition: state of the art

Vein pattern recognition systems employing finger veins [8], palm veins [9], hand dorsal veins [10], and wrist veins [11] have been proposed in literature, together with different approaches for the extraction of representative features from the network of blood vessels. Specifically, local or global statistical-based (SB) methods, using statistical features as the local binary histogram and moments, have been exploited to extract discriminative information from vein structures [12, 13]. Methods based on local binary patterns (LBPs) [14] and local derivative patterns (LDPs) [15] are worth to be mentioned among feature extraction techniques based on local statistics. Approaches relying on local invariant (LI) features, such as scale invariant feature transform (SIFT) [16, 17] or speeded-up robust features (SURF) [18, 19], have been also exploited. Subspace projections (SP), namely principal component analysis (PCA), linear discriminant analysis (LDA), non-negative matrix factorization (NMF), and independent component analysis (ICA), have been evaluated in literature too [20–22]. In addition, vein segmentation (VS) or minutiae and crossing points extraction have been applied for vein pattern processing [23].

In this work, we propose a biometric system relying on palm-vein features. Many works on such biometric trait have been proposed, and some of the most relevant ones are summarized in Table 1. In the aforementioned table, details of the employed database, as well as about the proposed feature extraction techniques, category and matching strategies, are reported together with the achieved recognition performance. The features exploited in this work to perform palm vein recognition are described in Section 4.4.

3 Vein patterns and high dynamic range

It is well known that blood hemoglobin absorbs NIR light. Therefore the vein pattern imaging is carried out through a NIR camera and a NIR illumination system. This latter has to be properly calibrated in order to allow the light to penetrate skin and tissues till reaching the blood vessels, which would appear as dark lines in the

Kindly cite this paper as: E. Piciucco, E. Maiorana, and P. Campisi, "Palm Vein Recognition Using a High Dynamic Range Approach", *IET Biometrics*, vol. 7, issue 5, pp. 439–446, Sept 2018, doi: 10.1049/iet-bmt.2017.0192

Table 1 Overview of state-of-the-art contributions in the field of palm vein recognition.

Reference	Database			Employed System			Performance
	DB Name	Palms	Samples	Categ.	Feat. Extract	Matching	
Mirmohamadsadeghi et al. [24]	CASIA V1.0 [25]	200	6	SB	LBP LDP	Histogram Intersection	CIR = 93.20% CIR = 97.00%
Kang et al. [13]	CASIA V1.0 [25] (left hands)	100	6	SB	Mutual foreground LBP Mutual foreground LBP	Chi-square distance Chi-square distance + SVM score fusion	EER = 2.53% EER = 0.267%
Tome et al. [26]	VERA Palmvein [26]	220	10	SB	LBP	Histogram intersection	EER = 3.75%
Pratiwi et al. [27]	CASIA V1.0 [25]	200	6	SB	LBP Rotation Invariant	Cosine Distance	CIR = 96% EER = 11.7%
Ladoux et al. [28]	Own	24	60	LI	SIFT	Euclidian distance	EER = 0.14%
Kang et al. [17]	CASIA V1.0 [25]	200	6	LI	RootSIFT	RootSIFT matching + LBP-based mismatching removal	EER = 0.996%
	Own	210	6		RootSIFT	RootSIFT matching + LBP-based mismatching removal	EER = 3.112%
Zhou et al. [16]	CASIA V1.0 [25]	200	6	SP	NMRT Hessian Phase	Hamming distance	EER = 0.51% EER = 0.44%
	PolyU [29]	500	12		NMRT Hessian Phase	Hamming distance	EER = 0.004% EER = 0.43%
Lee [30]	Own	207	20	SP	Modified $(2D)^2$LDA	Euclidian distance	CRR = 99.41%
Zhang et al. [31]	Own	24	6	VS	Matched filters	Hamming distance	EER = 4.00%
Lee et al. [9]	Own	207	20	VS	Adaptive Gabor filter	Normalized Hamming distance	EER = 0.44%
Wu et al. [32]	Own	256	20	VS	Gaussian filter bank	Normalized Hamming distance	EER = 0.518%
Wirayuda [33]	CASIA V1.0 [25] (left hands)	100	6	VS	Minutiae features	Weighted Euclidean distance	CIR = 90.87%
Cancian et al. [34]	Own	24	3	VS	2D Gabor filters	Hellinger distance	EER = 1.84%

acquired image. Unfortunately, vein structures are not evenly positioned under the skin with respect to the imaging and illumination devices, with the result that the obtained images may appear saturated if too much illumination power is employed, or dark if not enough illumination is used. Moreover, the transmittance of the NIR light across the different tissues of the hand is not uniform, due to the different thickness of bones and tissues. This results in veins from the thicker parts of the hand being less distinguishable compared to veins located in the thinner parts. Additionally, being standard camera sensors commonly able to handle only 8-bit images, the full luminance dynamic range cannot be sensed, thus producing low-contrast images with potential loss of details and useful information. Examples of the aforementioned issues are shown in Figs. 1 and 3. All these undesired effects impact on the quality of the captured vein pattern, leading to a degradation of the recognition accuracy in a biometric system. Thus, improving the quality of the captured vein images is a crucial task in a vein-based recognition system.

Different solutions have been proposed in order to face the aforesaid problems. Contrast enhancement techniques have been deeply investigated in literature as a solution to face the uneven illumination in the acquired vein pattern images [35, 36]. However, image enhancement is not able to recover the information loss due to either overexposure or underexposure of some regions of the picture. Therefore, several works about the adjustment of the illuminance distribution of the lighting system have been proposed [37, 38]. In detail, an uniform illumination in the acquired vein pattern image is obtained by adapting the light source during each image capture. The disadvantages of this kind of approach are that, being the light source modified each time, the system settings vary from acquisition to acquisition and the process of illumination adjustment is typically time consuming. Eventually, multimodal biometric fusion schemes have been extensively proposed in order to increase the system accuracy. Among them, multispectal image-level fusion, that is the combination of palm vein and palmprint images [22, 39], and feature-level fusion approaches [40] can be mentioned.

In order to counteract the aforementioned undesired effects, we propose a vein pattern recognition system performing information fusion at the sensor level, relying on HDR imaging techniques able to synthesize images with dynamic range far larger than the one representable in LDR images [7, 41]. The increase of dynamic range can be generated either directly capturing HDR images exploiting specialized devices, which are usually bulky and costly, or merging a set of single-exposure images acquired at different shutter speeds, namely using a bracketing-based approach. This latter allows reconstructing the original dynamic range and capturing details from both the image's brightest and darkest areas, taking details pertaining to dark areas from LDR pictures captured with high shutter speeds and contents from very bright regions from low-exposures pictures. The quality of the generated HDR content is therefore typically higher than what is present in its LDR counterpart.

4 Employed palm vein recognition system

4.1 Image Acquisition

The employed acquisition setup consists of a NIR camera and a NIR illuminator. During each registration a set of N LDR images is acquired at different shutter speeds. Examples of images acquired using our experimental setup are given in Figs. 1 and 3. Implementation details of the employed framework are given in Section 5.1.

4.2 Preprocessing

A region of interest (ROI) containing the palm vein pattern, with size 240×240, is first extracted from the acquired image. A non-linear image processing is then performed to face the issue of non-uniform background illumination and low contrast in vein pattern images. In detail, the ROI images are divided into blocks of 20×20 pixels, with 4-pixel overlap between two adjacent blocks. For each block the

Kindly cite this paper as: E. Piciucco, E. Maiorana, and P. Campisi, "Palm Vein Recognition Using a High Dynamic Range Approach", *IET Biometrics*, vol. 7, issue 5, pp. 439–446, Sept 2018, doi: 10.1049/iet-bmt.2017.0192

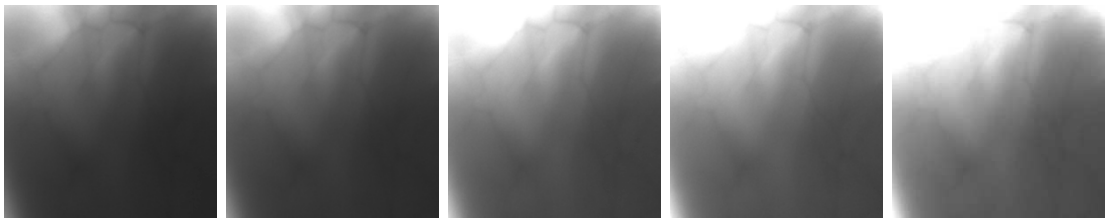

(a) (b) (c) (d) (e)

Fig. 1: Palm vein LDR images acquired with exposure time to (a) 0.036s (b) 0.042s (c) 0.048s (d) 0.054s (e) 0.060s.

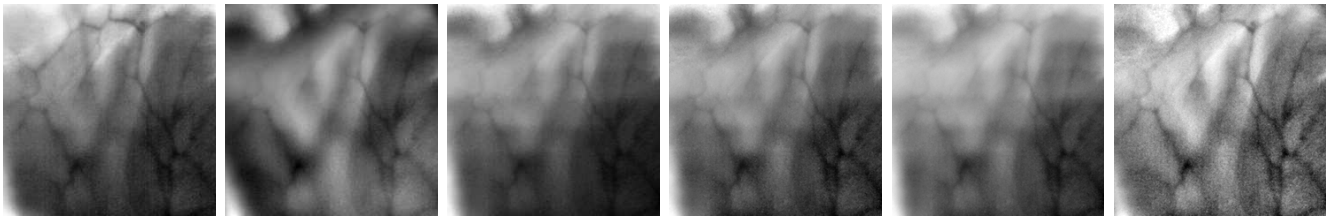

(a) (b) (c) (d) (e) (f)

Fig. 2: HDR vein images after (a) iCam06 [42] (b) Chiu [43] (c) Drago [44] (d) Ferbman [45] (e) Shan [47] (f) Shibata [48] tone mapping methods applied on the merged LDR images of Fig. 1.

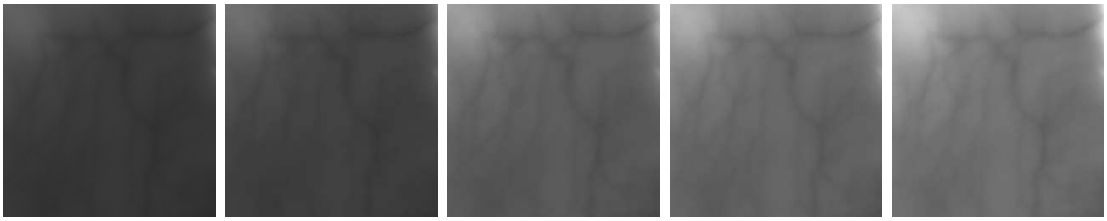

(a) (b) (c) (d) (e)

Fig. 3: Palm vein LDR images acquired with exposure time to (a) 0.036s (b) 0.042s (c) 0.048s (d) 0.054s (e) 0.060s.

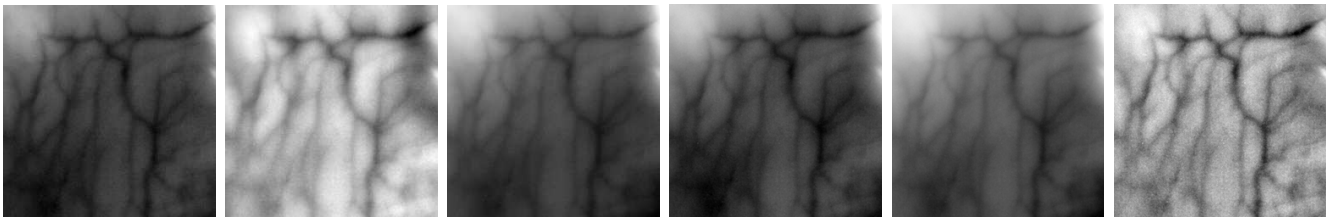

(a) (b) (c) (d) (e) (f)

Fig. 4: HDR vein images after (a) iCam06 [42] (b) Chiu [43] (c) Drago [44] (d) Ferbman [45] (e) Shan [47] (f) Shibata [48] tone mapping methods applied on the merged LDR images of Fig. 3.

average gray level is computed. The set of obtained mean values is then expanded into 20×20 blocks using a bicubic interpolation, generating the estimated background illumination. This latter is finally subtracted from the considered image, thus obtaining the enhanced vein pattern. We will refer to the described preprocessing method as background-removal (BR) preprocessing in the next sections.

4.3 HDR content generation

In order to generate the desired HDR vein pattern representation, the N different single-exposure images are combined through a weighted sum of their LDR luminance contents, taking into account the camera response function (CRF) and the exposure time of each picture [5]. The aim of the employed weighting function is to give more importance to middle luminance values while removing possible outliers. We refer to the image obtained by combining the LDR sources as raw HDR image.

The obtained HDR content can be later processed in order to properly represent the dynamic range on LDR devices, by means of tone mapping operators (TMO). Specifically, the aim of a TMO is to adapt the high dynamic range of the merged images to a low dynamic range device, still keeping details and contrast of the raw HDR data.

In this paper we apply several TMOs, specifically iCam06 [42], Chiu [43], Drago [44], Farbman [45], Reinhard [46], Shan [47], and Shibata [48], and evaluate the recognition performance on the so-obtained tone-mapped HDR images. Examples of tone-mapped HDR images, generated from the data shown in Figs. 1 and 3, are given respectively in Figs. 2 and 4.

4.4 Feature extraction

Two feature extraction approaches based on local textures, namely local binary pattern and local derivative pattern, are here used to obtain palm vein descriptors.

4.4.1 Local binary pattern: The LBP operator is a texture descriptor based on the gray level differences and comparisons of a neighborhood of pixels [15, 49]. Given a central pixel Z_0, an $R \times R$ neighborhood of P pixels is thresholded by the value of the central pixel and the LBP code for each center pixel of a greyscale image I is obtained as:

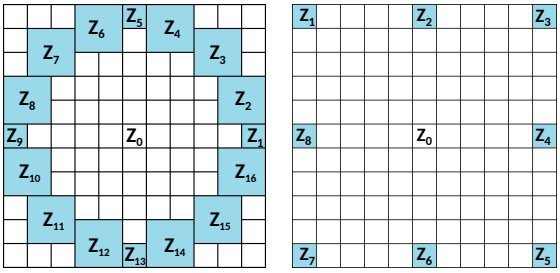

(a) (b)

Fig. 5: An example of (a) LBP and (b) LDP neighbourood

$$LBP_{P,R}(Z_0) = \sum_{p=1}^{P} f(Z_p, Z_0) 2^{p-1} \tag{1}$$

where Z_p is one of the P neighbors of Z_0, as shown in Fig. 5a. If the p^{th} neighbor is not a single pixel of the image, a weighted average of the selected pixels is performed, where the weights depend on the distance of the pixels with respect to Z_0. The thresholding function $f(Z_p, Z_0)$ can be represented as:

$$f(Z_p, Z_0) = \begin{cases} 0, & \text{if } I(Z_p) - I(Z_0) < 0 \\ 1, & \text{if } I(Z_p) - I(Z_0) \geq 0. \end{cases} \tag{2}$$

Each LBP code represents a micro-pattern of the image and it is saved in a histogram which contains information about the occurrence of the different kind of micro-pattern.

4.4.2 Local derivative pattern: The LDP operator is a high-order texture descriptor which extracts the derivative direction variation information [15, 50]. The directions considered to compute derivatives are 0°, 45°, 90° and 135°, where the derivatives along each direction are computed by subtracting pixels of a neighborhood according to the selected direction. In detail, the first-order derivatives along the four directions, with respect to a given central pixel Z_0, are computed as follows:

$$\begin{aligned} I'_{0^\circ}(Z_0) &= I(Z_0) - I(Z_4) \\ I'_{45^\circ}(Z_0) &= I(Z_0) - I(Z_3) \\ I'_{90^\circ}(Z_0) &= I(Z_0) - I(Z_2) \\ I'_{135^\circ}(Z_0) &= I(Z_0) - I(Z_1) \end{aligned} \tag{3}$$

where $Z_1, \ldots, Z_4$ are four of the neighbors around the center pixel chosen according to the direction of the derivative, as shown in Fig. 5b. For a given direction α and central pixel Z_0, the second order LDP code is encoded through the concatenation of the bits corresponding to each neighbor:

$$\begin{aligned} LDP^2_\alpha(Z_0) = \big\{ & f(I'_\alpha(Z_0), I'_\alpha(Z_1)), \ldots, \\ & f(I'_\alpha(Z_0), I'_\alpha(Z_8)) \big\} \end{aligned} \tag{4}$$

where the function $f(I'_\alpha(Z_0), I'_\alpha(Z_i))$ is a binary function providing the type of local pattern, defined as:

$$f(I'_\alpha(Z_0), I'_\alpha(Z_i)) = \begin{cases} 0, & \text{if } I'_\alpha(Z_0) \cdot I'_\alpha(Z_i) > 0 \\ 1, & \text{if } I'_\alpha(Z_0) \cdot I'_\alpha(Z_i) \leq 0\,, \end{cases} \tag{5}$$

where $i = 1, 2, \ldots, 8$ is the neighbor's index.

The obtained codes are converted into a decimal value and stored into an histogram which represents the image descriptor. This formulation can be generalized for the n^{th} order LDP, considering the $(n-1)^{th}$ order derivatives in the four directions in the computation of the LDP codes.

5 Experiments

5.1 Experimental setup

The palm vein database employed for our experimental tests is collected using a Visiosens VFU-V024-M-H-C NIR camera as acquisition device, and an array of NIR leds (wavelength = 850 nm) as illuminator. The resolution of the camera sensor is 752×480 pixels, with 8 bit gray-scale per pixel. The CCD camera sensitive range is between 450 and 900 nm and, in order to eliminate the effect of visible light, the B+W F Pro IR 093 optical infrared filter, with cut-on wavelength at 825 nm, is mounted in front of the camera's lens.

The acquisition process is carried out using a docking device for hand placement and ROI extraction, consisting of a window of the desired dimension and pegs for correct hand positioning, to reduce both misalignment and registration problems. The processed ROI consists of 240×240 pixels, corresponding to a vein width of about 2-8 pixels.

Data from 86 subjects are collected in the employed dataset. The right palm of each subject is acquired five times at exposure time $T \in \{0.036, 0.042, 0.048, 0.054, 0.060\}s$, entailing a total capture time of about $T_{tot} = 0.24s$. This process is iterated twelve times for each palm, thus obtaining a dataset of 86 users × 12 palms × 5 exposures.

Features are extracted from single-exposures images, from raw HDR image, and from tone-mapped HDR images, considering both the LBP and LDP extraction methods. In our tests, LBP features are extracted considering $P = 16$ neighbors and a neighborhood radius $R = 8$. The LBP operator is applied to 16 non-overlapping 60×60 blocks, with the LBP computed on $(2R+1)$ x $(2R+1)$ sub-blocks centered around each pixel of the block. The histograms resulting from the application of the LBP to each block consist of $P(P-1) = 240$ bins, then concatenated to generate the palm vein template. When LDP is applied, the second-order operator is chosen and a radius of 5 pixels from the central pixel is set when the feature extraction step is performed. The image is divided into 16 non-overlapping 60×60 blocks, and the derivatives in the four directions are computed for all the pixels of each block. The resulting LDP block histograms are concatenated to obtain the palm vein template, resulting of *number of blocks* · *number of directions* $\cdot 2^8$ = 16384 elements.

Given the so-computed templates, a matching score is obtained through the histogram intersection measure [51], defined as:

$$H(p, q) = \frac{\sum_i \min(p_i, q_i)}{\sum_i q_i} \tag{6}$$

where p and q are the two histograms to be compared, each one consisting of *i* bins, with $\sum_i q_i$ = 240·240.

HDR images are generated using both all the $N = 5$ images collected at different exposures, as well as only $N = 3$ of them, specifically the image at middle-exposure and the two having lower and the higher exposure time w.r.t. the middle one.

In order to perform a comprehensive analysis, we compare the performance of the proposed approach with what obtained when different image enhancement techniques are applied on the original LDR palm vein images. In detail, some proposed enhancement techniques for vein images are considered:

- histogram equalization (HE),
- contrast limited adaptive histogram equalization (CLAHE),
- circular gabor filter (CGF) [52],
- high-frequency emphasis filtering (HFE) [53],
- local-ridge-enhancement (LRE) [54],
- Retinex method (RM) [55].

The aforementioned techniques are applied to the originally acquired LDR images, which are then further preprocessed through the background-removal (BR) method, described in Section 4.2, thus

Kindly cite this paper as: E. Piciucco, E. Maiorana, and P. Campisi, "Palm Vein Recognition Using a High Dynamic Range Approach", *IET Biometrics*, vol. 7, issue 5, pp. 439–446, Sept 2018, doi: 10.1049/iet-bmt.2017.0192

Table 2 EER (%) obtained considering LBP and LDP feature extraction methods applied on the single middle-exposure image, on single-exposure images fused at score level, on raw HDR images and on tone-mapped HDR images.

	Middle Exposure	Exposures	Score Level Fusion	Raw HDR (no TMO)	iCam06 [42]	Chiu [43]	Drago [44]	Farbman [45]	Reinhard [46]	Shan [47]	Shibata [48]
LBP	3.81	5	3.63	2.97	2.65	**2.51**	2.97	2.99	2.98	2.96	2.59
		3	3.63	3.23	2.86	**2.71**	3.22	3.13	3.21	3.12	**2.51**
LDP	3.17	5	3.24	2.00	1.94	**1.74**	2.00	2.06	2.00	**1.74**	1.75
		3	2.97	2.06	2.19	**1.94**	2.13	2.19	2.07	2.06	2.06

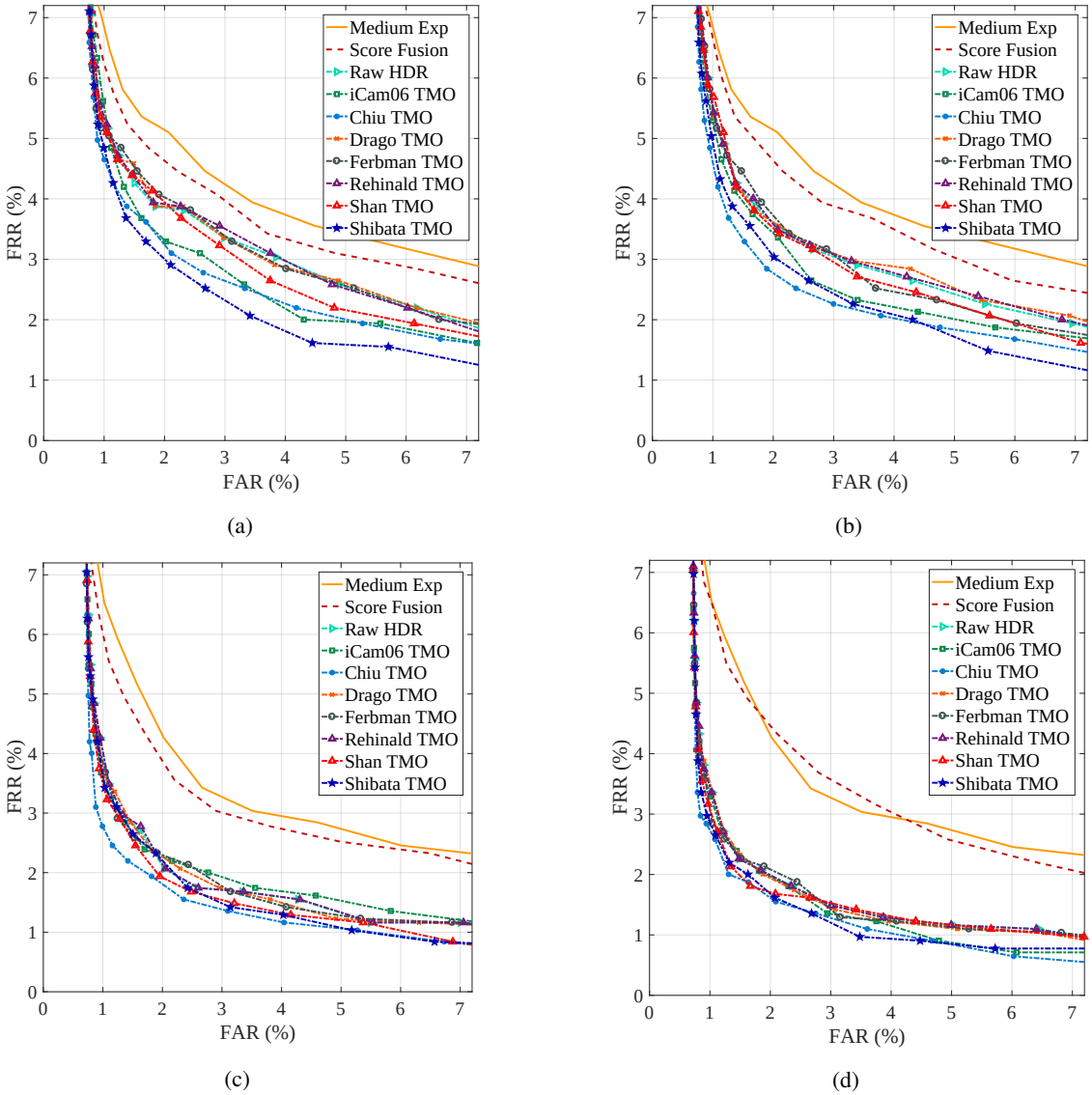

Fig. 6: DET curves obtained considering LBP features extracted from sets with (a) 3 and (b) 5 LDR images and considering LDP features extracted from sets with (c) 3 and (d) 5 LDR images.

obtaining the desired enhanced images. Finally, in order to have a performance comparison between the proposed approach based on sensor-level fusion and alternative information fusion methods, we also perform a score-level fusion approach [56] to combine the outputs obtained when matching features extracted either from the raw single-exposure images or from the enhanced vein images.

5.2 Experimental results

Tables 2 and 3 show the equal error rates (EERs) obtained when the LBP and LDP feature extraction methods are applied to the considered images. As first step, features extracted from each single-exposure image are matched in order to evaluate the performance for each considered exposure. The best performance is obtained when considering middle-exposure images, that is the image acquired when the exposure time is set to $T = 0.048$ s, with the achieved values reported in Table 2. The scores obtained from each single-exposure image are later combined following score-level fusion approaches, namely using the mean, minimum, and maximum rules. Sets with either 3 or 5 exposures have been exploited. The best results are obtained when the maximum between the scores is considered in the decision step, with corresponding values reported in Table 2. LBP and LDP operators are also applied to HDR data, before and after the application of the considered TMOs, with the obtained EERs reported in Table 2. Table 3 shows the results obtained when different vein image enhancement techniques, listed

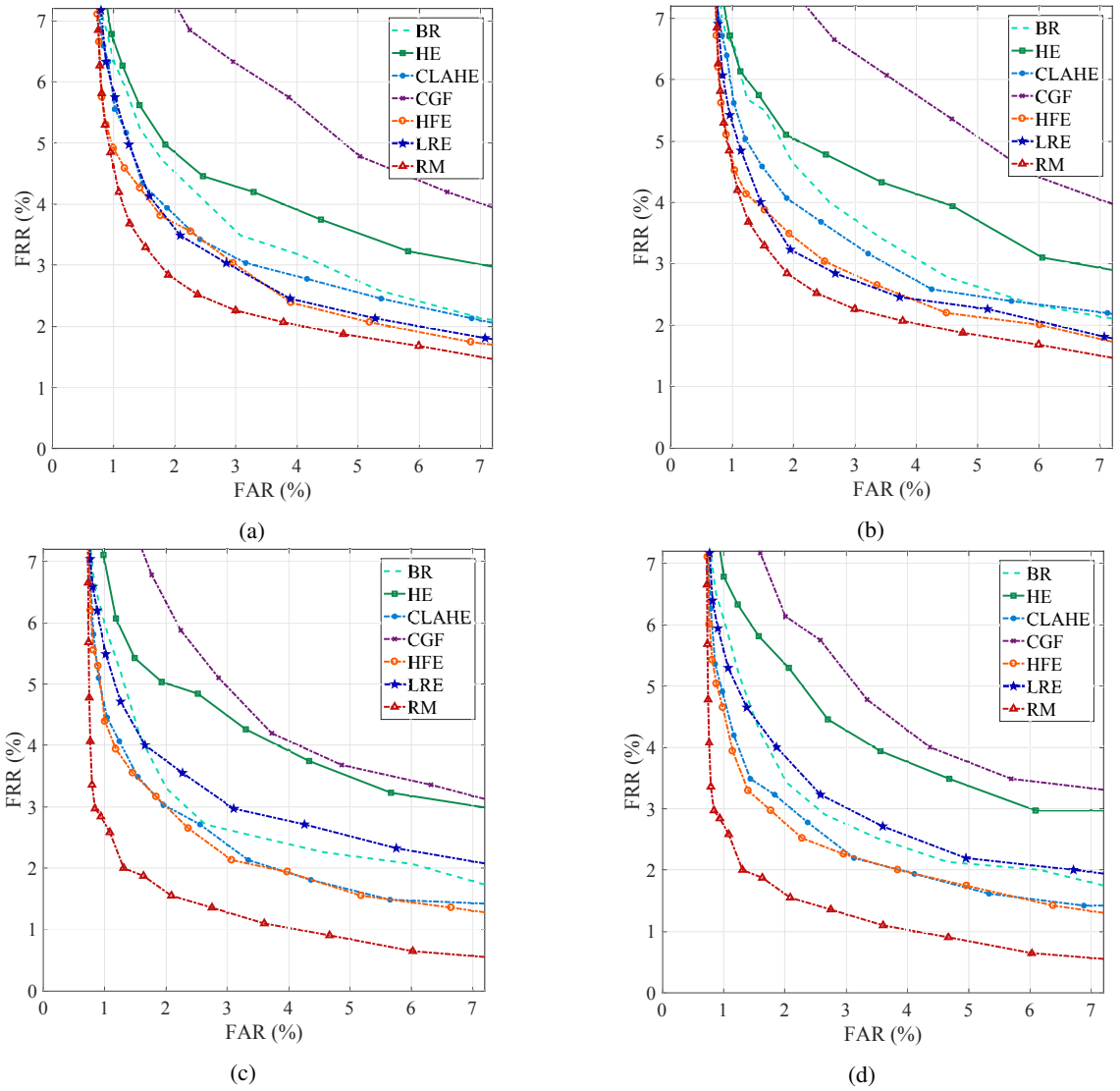

Fig. 7: DET curves obtained considering LBP feature extraction method applied on the enhanced vein images and then combining the scores of (a) 3 exposures (b) 5 exposures enhanced pictures and considering LDP feature extraction method applied on the enhanced vein images and then combining the scores of (c) 3 exposures (d) 5 exposures enhanced pictures.

Table 3 EER (%) obtained when LBP and LDP features are extracted only from the middle-exposure image preprocessed with the different image enhancement methods.

	BR	HE + BR	CLAHE + BR	CGF + BR	HFE + BR	LRE + BR	RM + BR
LBP	3.81	3.70	4.69	3.21	5.49	3.10	3.15
LDP	3.17	3.03	4.46	2.71	4.27	2.90	3.41

Table 4 EER (%) obtained considering the LBP and LDP features extracted from the enhanced LDR vein images and then performing a score-level fusion approach.

	Exposures	HE + BR	CLAHE + BR	CGF + BR	HFE + BR	LRE + BR	RM + BR
LBP	5	3.42	4.18	3.21	5.02	2.97	2.84
	3	3.38	3.54	3.10	4.90	3.03	2.91
LDP	5	2.71	3.81	2.59	4.16	2.45	2.91
	3	2.67	3.94	2.72	4.07	2.45	3.00

in Section 5.1, are applied to the middle-exposure image and, then, the background-removal (BR) preprocessing is performed. Besides, the performance regarding the score-level fusion approach applied to the results obtained from 3 or 5 exposures images enhanced with the considered preprocessing methods are presented in Table 4. In this case, we found out the mean rule being the best performing score-level fusion strategy. Finally, we performed additional tests to analyze the impact on performance of applying the aforementioned enhancement techniques to the LDR images to be fused and then performing the HDR approach applying the best performing TMO. The results obtained are not reported in this paper because no performance improvement is achieved in comparison to classical HDR approach. This was an expected behavior since the enhancement techniques modify the contrast of the LDR image and the HDR fusion process may not work correctly.

The detection error trade-off (DET) curves of systems based on middle-exposure images only, on score-level fusion of the available multi-exposure information, on raw HDR content, and on tone-mapped HDR data are also plotted in Fig. 6 for LBP and LDP features. When no HDR imaging techniques are considered, better recognition accuracy can be achieved when the image enhancement step is performed and the score-level fusion approach is then applied,

Kindly cite this paper as: E. Piciucco, E. Maiorana, and P. Campisi, "Palm Vein Recognition Using a High Dynamic Range Approach", *IET Biometrics*, vol. 7, issue 5, pp. 439–446, Sept 2018, doi: 10.1049/iet-bmt.2017.0192

Table 5 Acquisition and processing time (s) when the HDR imaging approach is considered.

Step		Required computational time 3 Exposures	5 Exposures
Image acquisition		0.1440 s	0.2400 s
Raw HDR image fusion		0.0176 s	0.0278 s
Tone mapping	iCam06 TMO [42]	0.1971 s	
	Chiu TMO [43]	0.3756 s	
	Drago TMO [44]	0.0058 s	
	Farbman TMO [45]	0.1444 s	
	Reinhard TMO [41]	0.0034 s	
	Shan TMO [47]	0.6133 s	
	Shibata TMO [48]	1.1158 s	

compared to the performance obtained when no combination of the scores is done. For this reason, only results of Table 4 are plotted in the DET curves of Fig. 7.

Eventually, we evaluated the increase in processing time when adopting the sensor-level-fusion strategy in comparison to the baseline system. Our experiments are performed on a Core i7-6800K CPU @ 3.40 GHz with 64.0 Gb of RAM and the algorithms are implemented in MATLAB. In detail, in our HDR-based approach additional time is required in the stages of image acquisition, fusion and possible tone mapping operation. The obtained performance is reported in Table 5, where the shown values represent the average times required to process all the images in the considered database.

It can be seen that extracting features from HDR images leads to significant recognition performance improvement, when adopting both LBP and LDP representations, with respect to processing the original single-exposure data. In particular, when the LBP feature extraction method is considered, an EER of 3.81% is obtained when the middle-exposure image is considered, while an EER of 2.51% is reached when the features are extracted from the HDR image built from 5 LDR images fused with the Chiu TMO [43] or when 3 LDR images are combined and then the Shibata TMO [48] is applied. Results concerning LDP features also confirm this behavior, showing an EER of 3.17% obtained when using only middle-exposure images, and an EER of 1.74% with tone-mapped HDR content generated with 5 images taken at different exposures, both considering the Chiu [43] and Shan [47] TMOs. The obtained results also show that generating HDR images considering 5 exposures instead of 3 leads to better results in most of the cases. As shown in Table 5, the best performing and less time consuming TMO is the Chiu operator and it is worth highlighting that, when the best performance is achieved, an average total additional time of $T_{proc} = 0.192$ s (acquisition of four additional LDR-images) + 0.0278 s (row HDR image generation) + 0.3756 s (Chiu TMO) = 0.5954 s is needed.

It is worth remarking that the employed sensor-level fusion approach based on HDR imaging always gives better results compared to the score-level fusion strategy. It is also important to stress out that, with respect to score-level fusion approach, exploiting sensor-level fusion gives additional advantages in terms of required storage space and computational cost. In fact, using HDR content requires extracting features only from a single image, while all the single-exposures images have to be taken into account in the feature extraction and matching stages when score-level fusion is implemented, with the further burden of storing all the derived templates. Finally, we also show that, using HDR imaging techniques, it is possible to achieve better results compared to what obtained when the vein images are enhanced by exploiting preprocessing techniques, both considering the score-level fusion approach and not taking it into account.

6 Conclusions

In this paper we have studied the impact on recognition performance of applying HDR imaging on palm vein recognition systems, performing a sensor-level fusion approach on images captured at multiple exposures. The obtained results show that significant performance improvement can be reached when HDR content is processed, compared to the use of single-exposure LDR vein images. Besides, the adoption of TMOs allows guaranteeing even further improvements, with performance notably exceeding those achieved when employing vein image enhancement methods and score-level information fusion approaches.

7 References

1 Jain, A. K., Ross, A., Prabhakar, S.: 'An introduction to biometric recognition', *IEEE Trans. on Circuits and Systems for Video Technology*, 2004, **14**, (1), pp. 4–20.
2 Miura, N., Nagasaka, A., Miyatake, T.: 'Feature extraction of finger-vein patterns based on repeated line tracking and its application to personal identification', *Machine Vision and Applications*, 2004, **15**, (4), pp. 194–203.
3 Piciucco, E., Maiorana, E., Kauba, C., Uhl, A., Campisi, P.: 'Cancelable biometrics for finger vein recognition', Proc. 1st Int. Workshop on Sensing, Processing and Learning for Intelligent Machines, July 2016, pp. 1–5.
4 Kauba, C., Piciucco, E., Maiorana, E., Campisi, P., Uhl, A.: 'Advanced Variants of Feature Level Fusion for Finger Vein Recognition', Proc. Int. Conf. of the Biometrics Special Interest Group, September 2016, pp. 1–7.
5 Banterle, F., Artusi, A., Debattista, K., Chalmers, A.: 'Advanced high dynamic range imaging: theory and practice', (CRC Press, 2011).
6 McCann, J. J., Rizzi, A.: 'The art and science of HDR imaging', Vol. 26., John Wiley & Sons, 2011.
7 Chalmers, A., Campisi, P., Shirley, P., Olaizola, I. G.: 'High Dynamic Range Video: Concepts, Technologies and Applications', (Academic Press, 2016).
8 Rosdi, B. A., Shing, C. W., Suandi, S. A.: 'Finger vein recognition using local line binary pattern', *Sensors*, 2011, **11**, (12), pp. 11357–11371.
9 Lee, J. C.: 'A novel biometric system based on palm vein image', *Pattern Recognition Letters*, 2012, **33**, (12), pp. 1520–1528.
10 Lin, C. L., and Fan, K. C.: 'Biometric verification using thermal images of palm-dorsa vein patterns', *IEEE Trans. on Circuits and Systems for Video Technology*, 2004, **14**(2), pp. 199–213.
11 Pascual, J. E. S., Uriarte-Antonio, J., Sanchez-Reillo, R., Lorenz, M. G.: 'Capturing hand or wrist vein images for biometric authentication using low-cost devices', Proc. 6th Int. Conf. on the Intelligent Information Hiding and Multimedia Signal Processing, October 2010, pp. 318–322.
12 Wang, Y., Li, K., Cui, J.: 'Hand-dorsa vein recognition based on partition local binary pattern', Proc. 10th Int. Conf. on Signal Processing, October 2010, pp 1671–1674.
13 Kang, W. and Wu, Q.: 'Contactless palm vein recognition using a mutual foreground-based local binary pattern', *IEEE Trans. on Information Forensics and Security*, 2014, **9**, (11), pp 1974–1985.
14 Lee, E. C., Lee, H. C., Park, K. R.: 'Finger vein recognition using minutia-based alignment and local binary pattern-based feature extraction', *Int. Journal of Imaging Systems and Technology*, 2009, **19**, (3), pp. 179–186.
15 Mirmohamadsadeghi, L., Drygajlo, A.: 'Palm vein recognition with local binary patterns and local derivative patterns', Proc. Int. Joint Conf. on Biometrics, October 2011, pp. 1–6.
16 Zhou, Y. and Kumar, A.: 'Human identification using palm-vein images', *IEEE Trans. on Information Forensics and Security*, 2011, **6**, (4), pp. 1259–1274.
17 Kang, W., Liu, Y., Wu, Q., Yue, X.: 'Contact-free palm-vein recognition based on local invariant features', *PloS one*, 2014, **9**, (5), pp. 97548.
18 Pan, M., Kang, W.: 'Palm vein recognition based on three local invariant feature extraction algorithms', Proc. Chinese Conf. on Biometric Recognition, December 2011, pp. 116–124.
19 Kauba, C., Reissig, J., Uhl, A.: 'Pre-Processing Cascades and Fusion in Finger Vein Recognition', Proc. Int. Conf. of the Biometrics Special Interest Group, September 2014, pp. 1–6.
20 Hsu, C. B., Hao, S. S., Lee, J. C.: 'Personal authentication through dorsal hand vein patterns', *Optical Engineering*, 2011, **50**, (8), pp. 087201–087201.
21 Liu, Z., Yin, Y., Wang, H., Song, S., Li, Q.: 'Finger vein recognition with manifold learning', *Journal of Network and Computer Applications*, 2010, **33**, (3), pp. 275–282.
22 Wang, J. G., Yau, W. Y., Suwandy, A., Sung, E.:'Person recognition by fusing palmprint and palm vein images based on "Laplacianpalm" representation', *Pattern Recognition*, 2008, **41**, (5), pp. 1514–1527
23 Kumar, A., Prathyusha, K. V.: 'Personal authentication using hand vein triangulation and knuckle shape', *IEEE Trans. on Image Processing*, 2009, **18**, (9), pp. 2127–2136.
24 Mirmohamadsadeghi, L., Andrzej D.: 'Palm vein recognition with local texture patterns', *IET Biometrics*, 2014, **3**, (4), pp. 198–206.
25 "CASIA Multi-Spectral Palm Print Image Database V1.0", Chinese Academy of Sciences Institue of Automation (CASIA), [Online]. Available: `http://biometrics.idealtest.org/`.
26 Tome, P., Marcel, S.: 'Palm vein database and experimental framework for reproducible research', Proc. Int. Conf. of the Biometrics Special Interest Group, September 2015, pp. 1–7.
27 Pratiwi, A. Y., Budi, W. T. A., Ramadhani, K. N.: 'Identity recognition with palm vein feature using local binary pattern rotation Invariant', Proc. 4th Int. Conf. on Information and Communication Technology, May 2016, pp. 1–6.
28 Ladoux, P. O., Rosenberger, C., Dorizzi, B. 'Palm Vein Verification System Based on SIFT Matching', Proc. 3rd Int. Conf. on Biometrics, June 2009, pp. 1290–1298.
29 Zhang, D., Guo, Z., Lu, G., Zhang, L., Zuo, W.: 'An online system of multispectral palmprint verification', *IEEE Trans. on Instrumentation and Measurement*, 2011, **59**, (2), pp. 480–490.

30 Lee, Y. P.: 'Palm vein recognition based on a modified $(2D)^2$LDA', *Signal, Image and Video Processing*, 2015, **9**, (1), pp. 229–242.
31 Zhang, Y. B., Li, Q., You, J., Bhattacharya, P.: 'Palm vein extraction and matching for personal authentication', *Advances in Visual Information System*, 2007, pp. 154-164.
32 Wu, K. S., Lee, J. C., Lo, T. M., Chang, K. C., Chang, C. P.: 'A secure palm vein recognition system', *Journal of Systems and Software*, 2013, **86**, (11), pp. 2870–2876.
33 Wirayuda, T. A. B.: 'Palm vein recognition based-on minutiae feature and feature matching', Proc. Int. Conf. on the Electrical Engineering and Informatics, August 2015, pp. 350–355.
34 Cancian, P., Di Donato, G. W., Rana, V., Santambrogio, M. D.: 'An embedded Gabor-based palm vein recognition system', Proc. Int. Conf. on Biomedical & Health Informatics, February 2017, pp. 405–408.
35 Yang, J., Yang, J.: 'Multi-channel gabor filter design for finger-vein image enhancement', Proc. 5th Int. Conf. on Image and Graphics, September 2009, pp. 87–91.
36 Djerouni, A., Hamada, H., Loukil, A., Berrached, N.: 'Dorsal hand vein image contrast enhancement techniques', *Int. Journal of Computer Science*, **11**, (1), 2014, pp. 137–142.
37 Xu, J., Jianjiang, C., Dingyu, X., Feng, P.: 'Near infrared vein image acquisition system based on image quality assessment', Proc. Int. Conf. on Electronics, Communications and Control, September 2011, pp. 922–925.
38 Chen, L., Wang, J., Yang, S., He, H.: 'A Finger Vein Image-Based Personal Identification System With Self-Adaptive Illuminance Control', *IEEE Trans. on Instrumentation and Measurement*, 2017, **66**, (2), pp. 294-304.
39 Hao, Y., Sun, Z., Tan, T., Ren, C.: 'Multispectral palm image fusion for accurate contact-free palmprint recognition', Proc. 15th IEEE Int. Conf. on Image Processing, October 2008, pp. 281–284.
40 Yan, X., Kang, W., Deng, F., Wu, Q.: 'Palm vein recognition based on multi-sampling and feature-level fusion', *Neurocomputing*, 2015, **151**, (2), pp. 798–807.
41 Reinhard, E., Heidrich, W., Debevec, P., Pattanaik, S., Ward, G., Myszkowski, K.: 'High dynamic range imaging: acquisition, display, and image-based lighting', (Morgan Kaufmann, 2010).
42 Kuang, J., Johnson, G. M. Fairchild, M. D.: 'iCAM06: A refined image appearance model for HDR image rendering', *Journal of Visual Communication and Image Representation*, 2007, **18**, (5), pp. 406–414.
43 Chiu, K., Herf, M., Shirley, P., Swamy, S., Wang, C., Zimmerman, K.: 'Spatially nonuniform scaling functions for high contrast images', *Graphics Interface*, 1993, pp. 245–245.
44 Drago, F., Myszkowski, K., Annen, T., Chiba, N.: 'Adaptive logarithmic mapping for displaying high contrast', *Computer Graphics Forum*, 2003, **22**, (3), pp. 419–426.
45 Farbman, Z., Fattal, R., Lischinski, D., Szeliski, R.: 'Edge-preserving decompositions for multi-scale tone and detail manipulation', *ACM Transactions on Graphics*, 2008, **27**, (3), p. 67.
46 Reinhard, E., Stark, M., Shirley, Pe., Ferwerda, J.: 'Photographic tone reproduction for digital images', *ACM Trans. on Graphics*, 2002, **21**, (3), pp. 267–276.
47 Shan, Q., Jia, J., Brown, M. S.: 'Globally optimized linear windowed tone mapping', *IEEE Trans. on Visualization and Computer Graphics*, 2010, **16**, (4), pp. 663–675.
48 Shibata, T., Tanaka, M., Okutomi, M: 'Gradient-Domain Image Reconstruction Framework with Intensity-Range and Base-Structure Constraints', Proc. IEEE Conf. on Computer Vision and Pattern Recognition, June 2016, pp. 2745–2753.
49 Ojala, T., Pietikainen, M., Harwood, D.: 'Performance evaluation of texture measures with classification based on Kullback discrimination of distributions', Proc. 12th Int. Conf. on Computer Vision & Image Processing, 1994, pp. 582–585.
50 Zhang, B., Gao, Y., Zhao, S., Liu, J.: 'Local derivative pattern versus local binary pattern: face recognition with high-order local pattern descriptor', *IEEE Trans. on Image Processing*, 2010, **19**, (2), pp. 533–544.
51 Swain, M. J., Ballard, D. H.: 'Color indexing', *Int. Journal of Computer Vision*, 1991, **7**, (1), pp. 11–32.
52 Zhang, J., Yang, J.: 'Finger-vein image enhancement based on combination of gray-level grouping and circular gabor filter', Proc. Int. Conf. on Information Engineering and Computer Science, December 2009, pp. 1–4.
53 Zhao, J., Tian, H., Xu, W., Li, X.: 'A new approach to hand vein image enhancement', Proc. 2nd Int. Conf. on Intelligent Computation Technology and Automation, October 2009, pp. 499–501.
54 Michael, G. K. O., Teoh, A. B. J., Connie, T.: 'A contactless biometric system using palm print and palm vein features', (INTECH Open Access Publisher,2011).
55 McCann, J.: 'Lessons learned from mondrians applied to real images and color gamuts', *Color and Imaging Conference*, 1999, **1999**, (1), pp. 1–8.
56 Ross, A. A., Nandakumar, K., Jain, A.: 'Handbook of multibiometrics', (Springer Science & Business Media, 2006).

Kindly cite this paper as: E. Piciucco, E. Maiorana, and P. Campisi, "Palm Vein Recognition Using a High Dynamic Range Approach", *IET Biometrics*, vol. 7, issue 5, pp. 439–446, Sept 2018, doi: 10.1049/iet-bmt.2017.0192